Instrumentation to Measure the Depth/Time Fluctuations in Acoustic Pulses Propagated through Arctic Internal Waves

TERRY E. EWART* AND STEPHEN A. REYNOLDS

Applied Physics Laboratory, College of Ocean and Fishery Sciences, University of Washington, Seattle, Washington

(Manuscript received 25 May 1989, in final form 22 August 1989)

ABSTRACT

Instrumentation for measuring the evolution of volume-scattered acoustic signals in both depth and time is described. Measurements were taken for 12 days during the spring of 1985 with transmitters and receivers suspended beneath arctic pack ice in the Beaufort Sea. These acoustic measurements were made simultaneously with extensive oceanographic measurements taken by other investigators during the Arctic Internal Wave Experiment (AIWEX). A depth cycling vertical array of three receivers and a single fixed horizontal receiver 100 m transverse to the propagation path were deployed 6.43 km from moored transmitters. A vertical depth cycle of 51 m produced a synthetic vertical aperture of 153 m. Pulses spanning three octaves in acoustic frequency (2, 4, 8, 16 kHz) were used. The scattered field was sampled more often at 8 and 16 kHz to assure sufficient sampling (better than Nyquist) of the space/time fluctuations. Ten Gbytes of acoustic pulse receptions were recorded on optical disk for later processing. The measurements provide a unique two-dimensional (space/time) dataset for testing theories of acoustic volume scattering due to internal waves and finestructure.

1. Introduction

Over time and space scales of hours to days and meters to kilometers, oceanic internal waves are the dominant scattering mechanism of acoustic energy transmitted in the broad frequency range of 100 Hz to 20 kHz. Moreover, internal waves and the steppy nonwavelike variability often called "finestructure" are ubiquitous in the ocean. Over the past two decades, several measurements have been made of acoustic variability in pulses transmitted over kilometer ranges in the ocean (for example, see Ewart 1976; Worcester et al. 1981; Ewart and Reynolds 1984; Reynolds et al. 1985). These measurements tested propagation theories where internal wave and finestructure statistics characterize the scattering medium. Usually fixed or relatively fixed experimental geometries were employed, the theoretical assumption being that each pulse transmission encounters a fixed snapshot of the intervening oceanic environment. Repeated acoustic transmissions then measure the temporal variability in the acoustic fluctuation statistics. The spatial variability of the medium is the actual scattering mechanism, and the evolution of the spatial index of refraction field in time is the observation. Because it is the spatial variability that scatters each pulse, a measurement in both depth and time is required to fully test acoustic volume-scattering theories. In this paper, we describe instrumentation used to make such a measurement beneath the arctic pack ice.

In the open ocean, the observation of acoustic travel times and amplitudes over a large depth span is difficult. For example, observations during the Mid-Ocean Acoustic Transmission Experiment, MATE (Ewart and Reynolds 1984) and the Cobb71 Experiment (Ewart 1976) were made at a few spatially separated points (four during MATE and three during Cobb71). In both experiments, towers were placed on seamounts to provide the rigidity required to measure the acoustic phase to a small fraction of a wave period. These experiments, however, did not provide sufficient spatial fluctuation measurements.

In the experiment described here, measurements of the two-dimensional (time and depth) variability of acoustic signals were made using a depth cycling set of transducers receiving pulses from a multifrequency transmitter 6.43 km away. The transmitter and receivers were suspended beneath arctic pack ice in the Beaufort Sea. These measurements were made during the AIWEX Acoustic Transmission Experiment (AATE) in the spring of 1985 as part of the Arctic Internal Wave Experiment (AIWEX). The latter was conducted by investigators from several institutions, the goal being the observation of oceanic internal waves in a low-energy environment—under arctic pack ice.

AIWEX provided the opportunity, given the stable

* Also associated with the School of Oceanography, University of Washington.

Corresponding author address: Dr. Terry E. Ewart, Applied Physics Laboratory, University of Washington, 1013 N.E. 40th St., Seattle, WA 98105-6698.

ice platform from which transmitters and receivers could be suspended, to measure the acoustic variability in both depth and time. The environmental measurements made by the AIWEX investigators provide the model statistics needed for input to acoustic fluctuation theory. The statistics predicted by theory are compared with the observed acoustic fluctuation statistics (this is known as the forward or direct problem). Eventually we hope to fully invert the acoustic measurements and obtain the statistics of the ocean sound speed field.

2. Experiment overview

The measurement goal of AATE was to obtain acoustic amplitude and travel time fluctuation statistics in both depth and time for testing predictions from wave propagation theories. The specific scientific goals addressed by this research include the following:

- in a forward sense, compare the acoustic fluctuations at a receiver due to arctic internal wave and finestructure variability with predictions;
- in an inverse sense, study the periodic and stochastic nature of arctic environmental processes by using the fact that a wave propagating in a weakly scattering medium carries with it a "memory" of the medium statistics;
- study how internal wave motions and oceanic finestructure limit our ability to locate sources using acoustic receiving arrays; and
- study the influence that surface scattering from the ice canopy has on the spatial fluctuations in the acoustic field.

Studies of ocean acoustic fluctuations differ from other problems in wave propagation in random media in that the statistics of the fluctuating medium are measurable. AATE took place during the environmental[1] sampling program conducted at the AIWEX ice camp. The environmental variability was well sampled in space and time. Because the expected fluctuations dictated the design of AATE, we briefly review AIWEX, provide an overview of the AATE component, and conclude the section with a summary of some of the environmental results relevant to the acoustic measurements.

AIWEX was conducted in the spring of 1985 in the Beaufort Sea north of Prudoe Bay, Alaska. The AIWEX environmental sampling program began on 20 March and was concluded on 3 May with camp evacuation. The camp layout is shown in Fig. 1a, and the drift track of the camp during the data-taking phase of AATE is shown in Fig. 1b. The camp included investigators from several institutions making measurements over a broad range of temporal and spatial scales (e.g., Levine et al. 1987; Padman and Dillon 1987).

To predict the acoustic propagation statistics, the statistics of the environmental field must be known. In general, stochastic models are employed [e.g., for internal waves the Garrett and Munk model or a variant is traditionally used (Munk 1981; Levine 1983)]. Parameters in the model are obtained from the local measurements and require spatial and temporal series. Ideally several types of measurements are made so that model statistics can be checked for consistency between the measurements. This is the case with AIWEX. Both moored time series and vertical series of sound speed and current velocity were obtained by the AIWEX investigators (Levine et al. 1987).

The AATE acoustic measurements began on 7 April and concluded 18 April. The AATE components of AIWEX (Fig. 1a) consisted of a hut near the AIWEX main camp that housed the receiving hardware and computer, and a remote transmitter site located about 6.4 km to the southeast. The receiver hut, about 0.3 km from the AIWEX main camp, also served to house the AATE personnel.

The ice deployment is both a constraint and an asset. Physical constraints in an ice camp environment require that equipment be portable and easily deployed using man power. On the positive side, the ice acts as a stable platform for suspending equipment. In AATE, our equipment consisted of a set of transmitting transducers with associated electronics; a set of receiving transducers and receiving electronics, with digitizing and data storage; and accurate, stable clocking. In addition to these components for making temporal acoustic measurements, we used a low-noise winch in taking measurements of the vertical acoustic field. A vertical array of receivers was cycled in depth to make the spatial measurement. The winch/cable combination was designed to generate little if any acoustic noise during the data-taking (down) phase of the cycle. The winch was provided by Marconi Underwater Systems of Cambridge, England.

At the remote site, the transmitter consisted of an electronics bottle suspended at depth just above four transducers. Four acoustic frequencies coherent with pulse repetition and pulse sampling rates were used (2.083, 4.166, 8.333, and 16.666 kHz—nominally 2, 4, 8, and 16 kHz). These three octaves sampled a broad range of scattering parameters. With the available power, 16 kHz was the highest frequency which we could use that would overcome chemical absorption over the AATE range. The details of the transmitter and receiver equipment are given in the next section.

The vertical receiving array consisted of three transducers equally spaced on a cable driven over repeated depth cycles using the winch. The deployed configuration consisted of four vertically spaced transducers. The bottom transducer, however, failed during launch,

[1] The word environmental is used to distinguish the measurements made by the AIWEX environmental program from the acoustic propagation measurements made in AATE.

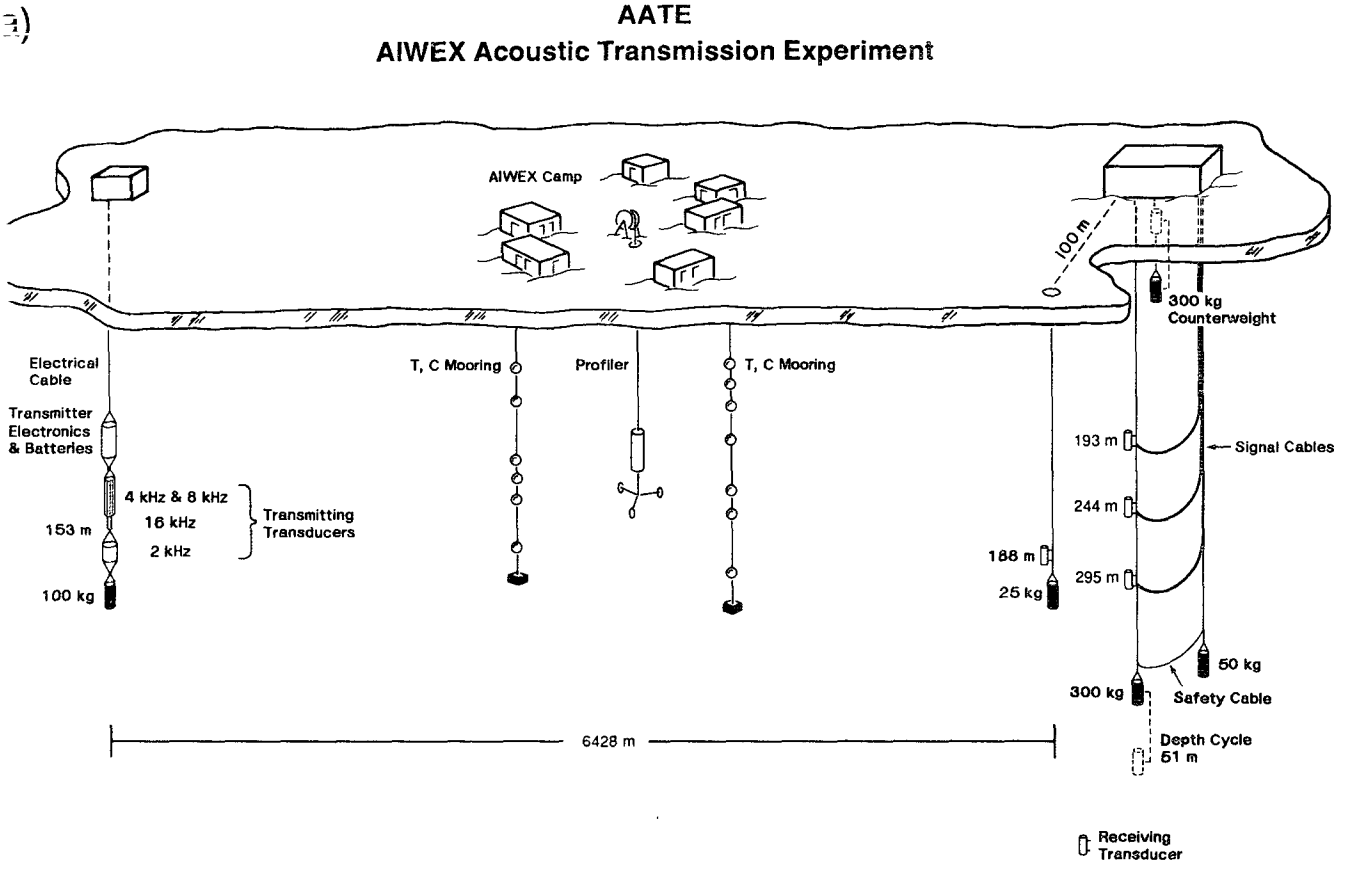

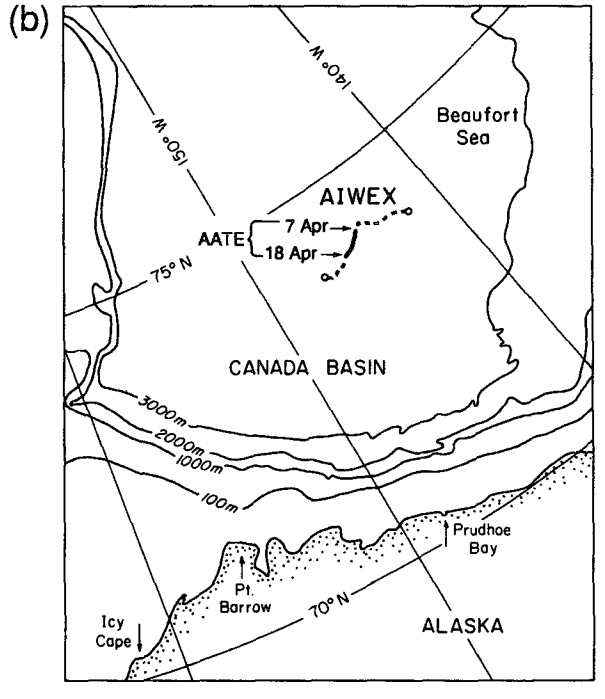

FIG. 1. A diagrammatic view of AATE is shown in (a). Note that the receiver hut at the right in (a) was actually about 0.3 km NNW of the AIWEX main camp. The remote transmitter hut, depicted at left, was about 6.4 km SSE of the main camp. The location of the ice camp during AIWEX is shown dashed in (b) (from Padman and Dillon 1987). The location of the camp during the AATE data-taking phase is shown as a solid line.

so the fourth data channel was used to record pulses at a fixed transducer placed 100 m transverse to the vertical array. This fixed transducer was suspended at 188 m depth and allowed a single horizontal sampling of the transverse acoustic field.

Sampling of the acoustic field was established during the planning stages of the experiment by anticipating the scattering regime from earlier measurements in the Arctic (Levine et al. 1985). These measurements demonstrated that the internal wave energy levels would be lower than those observed under open-ocean conditions. Measurements made at Cobb Seamount during the MATE (Ewart and Reynolds 1984) served as a guide to estimate the coherence times and spatial scales for sampling. An internal-wave energy level a factor of 10 lower than MATE was used. Because AATE was planned for a shallower deployment where the buoyancy frequency is higher, the effect of the lower internal wave energy was canceled by the increase in the local buoyancy frequency. Hence the index of refraction fluctuation levels due to internal waves were expected to be similar to those observed at the MATE site.

Given the estimated fluctuation level, the temporal and spatial decorrelation scales could be calculated from theory (Uscinski 1985). For the large end of the spatial scale, the spatial sampling needed to be at least a vertical correlation length of internal waves (about 100 m) and temporally sampled for as long as practical. The internal wave decorrelation time and space scales for 16 kHz were estimated to be 10 minutes and 2.5 m, respectively. (Finestructure scales are expected to be similar.) For 2 kHz, the vertical decorrelation scale estimate was 20 m.

With the sampling scale a function of acoustic frequency, the equipment needed to sample at a rate equal to half or one-fourth the smallest estimated scale for each acoustic frequency. Because this rate is a function of acoustic frequency, the pulses were transmitted in the sequence 2, 16, 8, 16, 4, 16, 8, 16. The vertical array needed to be driven at a relatively slow speed during the data-taking cycles in order to keep generated acoustic noise to a minimum. The temporal constraints meant the winch needed to return the 16 kHz transducers to their starting place at least every 5 minutes to avoid the temporal decorrelation limit. With a transducer separation of 51 m, the full depth span was sampled with the winch driven at a speed of 0.26 m s^{-1} during down cycles. To sample the 16 kHz at vertical scales at least half the decorrelation scale of 2.5 m, a basic transmission period of $\Delta t = 0.49152$ s was established. Thus the 16 kHz was sampled every $2\Delta t \times 0.26$ m $s^{-1} = 0.2556$ m. Over a full down cycle, 400 pulse samples were recorded from each transducer for a total time of 3.28 minutes. This allowed over 1½ minutes to return the winch to its rest position and start it down so the receivers would be moving at the proper speed at the starting time and position of the next sampling cycle. These rates satisfied the anticipated Nyquist criteria in space and time. Note that the acoustic pulse center frequencies are integral multiples of Δt^{-1}.

All receiver electronics, time windowing, pulse digitization, and winch operation were under the control of a single computer—a Masscomp MC5500 with an integral data acquisition system, control hardware, and software. Each of the four channels of pulse data was received and digitized every 15 μs; 1024 digitized samples were then recorded from each channel. With 3.2 Mbytes of data recorded for each cast, the total equaled nearly 10 Gbytes over the 12-day period. To store the data for post-experiment analysis, the received data were written to an Optimem optical disk drive having 1 Gbyte of storage per removable cartridge.

Before turning to a detailed hardware description, we briefly review results from the internal wave measurements. The measurements reported by Levine et al. (1987) were taken from current and temperature sensors moored in two triangular grids. The interior triangle carried a relatively dense suite of instruments. Simultaneously with the moored measurements, Morison and Andersen sampled the vertical variability with repeated casts of the Advanced Profiling System (Morison 1989). AIWEX temperature observations indicate an energy level of the internal wave field a factor of 0.03 to 0.07 of lower latitude, open-ocean measurements (Levine et al. 1987). In addition, the temporal frequency dependence is quite different from the traditional GM model. The consequences for the acoustic observations will be treated in future publications; here we only note that the energy level is around a factor of 20 lower than open-ocean values. The additional environmental variables needed to characterize the propagation environment are the "background" average sound speed and buoyancy frequency profiles. These were obtained from the vertical measurements of Morison and Andersen. From the background sound speed profile, a ray trace was calculated and is shown in Fig. 2. The ray angles near the transmitter and receiver are relatively steep (around 8°). There is no apparent multipathing. Details of the ray prediction will be a strong function of how the background sound speed profile was obtained. However, the qualitative nature of the received intensity pattern can be inferred from the trace in Fig. 2. Even though the rays are shot at equal angular increments, the rays are not equally spaced at the receiver plane, indicating that the background average intensity profile varies over the depth spanned by the receivers.

The rays shown in Fig. 2 depict the acoustic field of interest for the study of the forward and inverse volume-scattering problems. Note that the source/receiver depths and range separation were selected to avoid contamination of the volume arrival by the energy reflected from the ice canopy. The ice reflections arrive tens of milliseconds after the volume arrival and are gated out for the study of volume scattering.

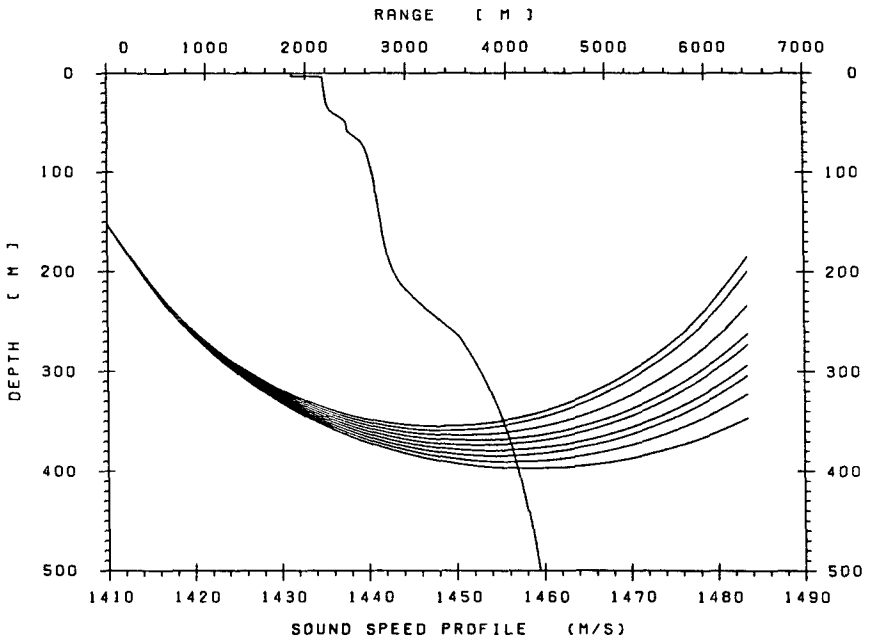

FIG. 2. Raytrace of the sound field over the 6.43 km AATE range. The transmit ray angles are from 7.95° to 8.35° with a uniform spacing of 0.05°. The sound speed profile used to calculate the raytrace is overplotted, with the scale shown along the bottom axis. The profile is from a 3-day average of casts taken during the middle of AATE with the Advanced Profiling System of Jamie Morison at the University of Washington.

3. Equipment

The AATE hardware elements consisted of the transmitter assembly, receiving array, winch, computer that controlled the receiving elements, and accurate clocks to ensure phase coherence between the transmitter and receiver. Because accurate measurement using acoustic techniques relies on stable clocking, we begin with the clocks. This is followed by a discussion of the transmitter and receiver/winch hardware. The section ends with a description of the computer data acquisition, storage, and control system. Much of the transmitter and receiver hardware had been used in 1977 during MATE (Ewart and Reynolds 1984; Reynolds 1982).

a. Clocks

Phase stability between the transmitter and receiver was maintained with 5 MHz Austron clocks housed in temperature stabilizing double ovens. The clock in the receiver hut was termed the master, and the transmitter clock, the slave. The clocks had not been run-in long enough to achieve the lowest possible drift rates, so the drift was measured during AATE. A radio link between the transmitter and receiver hut was used to monitor the drift between the two clocks. The clocks were synchronized at the beginning of the experiment (day 97). Drift measurements using the radio link began on day 101 and continued through the experiment. Figure 3 shows the relative drift between the clocks during the 12-day experiment. A cubic spline fit is shown as dashed.

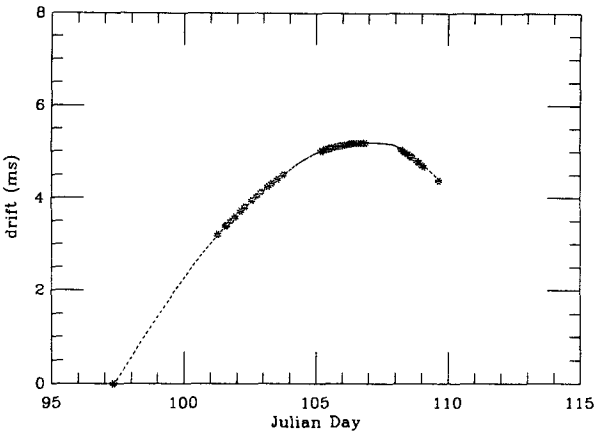

FIG. 3. Measurements of the relative drift during AATE. Two Austron oscillators maintained the phase accuracy between the transmitter and receiver. Sync information was telemetered between the remote transmitter hut and the master clock at the receiver. (The two clocks could be resynchronized over this link.) The base 5 MHz signal was divided down to the required digitization and pulse transmission rates. At the beginning of the experiment, the two clocks were synchronized and then their relative drift was monitored through the radio link. The relative drift measured between the two clocks is shown with asterisks in the diagram (the transmitter clock is ahead). A cubic spline fit to the drift data is shown as a dashed line.

In both slave and master clocks the 5 MHz oscillator frequency was divided down, first by 75 and then by 2^{15}, to get the basic sampling rate. The first division was the 15 microsecond pulse digitization rate and the second the 0.49152 s pulse repetition rate. The computer data acquisition and control clocking frequencies were obtained from the master clock. The timing is discussed further in the computer hardware section below.

b. *Transmitter*

A block diagram of the transmitter hardware is shown in Fig. 4. There were three items at the surface: the deployment winch; a power generator that recharged the batteries in the electronics bottle through a control box at the surface; and the radio transmitter for monitoring the signal transmissions and clocking at the main hut. The transmitting transducers and electronics bottle were all suspended below the ice, with the 16 kHz transducer deployed at a depth of 153 m.

Transmit/receive angles were a major concern in designing the arrays at AATE. The sources and receivers needed relatively wide beam patterns because the transmission angles were near 8°. The 4 and 8 kHz transducers consisted of five and three elements, respectively, with a spacing of 9.94 cm between elements. The 16 kHz transducer is a two-element array with a spacing of 8.26 cm. The 4, 8, and 16 kHz transducers are lead titanate zirconate cylinders encapsulated in polyurethane [EDO Western 249-5 (4 and 8 kHz) and 249-17 (16 kHz)]. The 2 kHz transducer is a single oil-filled ring consisting of a neoprene boot covering two active cylindrical elements [EDO Western 415-1.5]. The 4, 8, and 16 kHz elements were arranged in an axial array suspended with the electronics housing on an armored coaxial cable.

In the transmitter, pulse selection and generation were under digital control. Once the frequency was selected, a pulse was downloaded from PROM (Programmable Read-Only Memory), passed through a D/A converter, and sent to a driver and power amplifier for transmission from the appropriate transducer.

Several options for pulse shape and length were recorded in the PROM and available through the control box at the surface. The final pulses selected during AATE were 2 ms pulsed tones. With our pulse analysis technique, it was necessary to record the pulses at short range and "propagate" these ideal (unscattered) pulses out to the final range by modifying the pulses for the effects of geometric spreading and chemical absorption. [The equation of Francois and Garrison (1982) was used.] These single path, ideal pulse "replicas" are shown in Fig. 5.

c. *Winch and receiving array*

The receiving array was suspended from a winch cable that was driven over the element separation distance of 51 m by the Marconi low-vibration, counter-

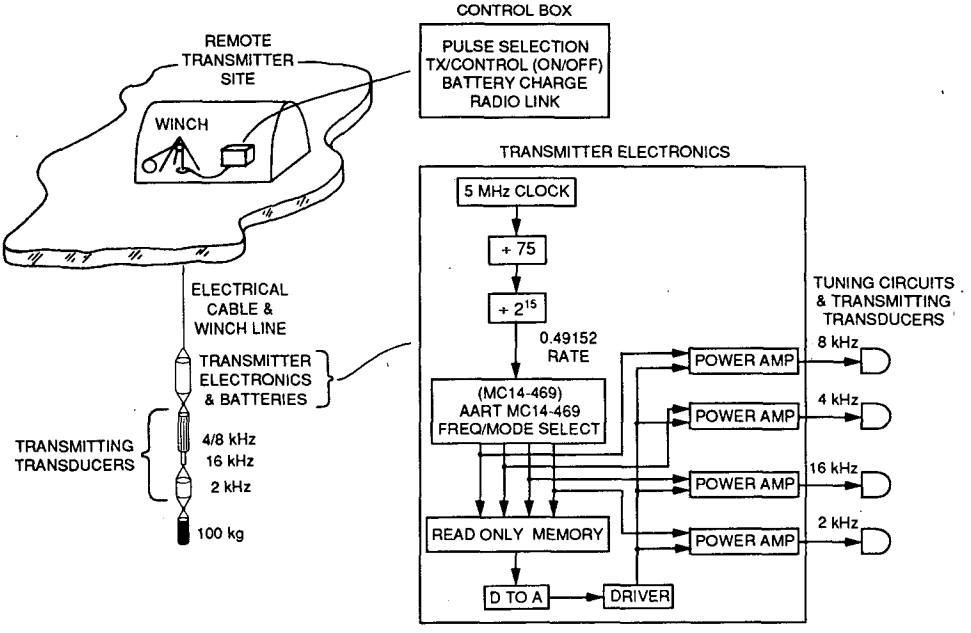

FIG. 4. Diagram of the transmitter showing the remote site and block diagrams of the electronics. The control box inside the remote hut allowed selection of eight pulse programs for four frequencies that control pulse length, ramp-up, and ramp-down. The selection used an addressable asynchronous receiver/transmitter (AART) to control programmable memory in the transmitter electronics.

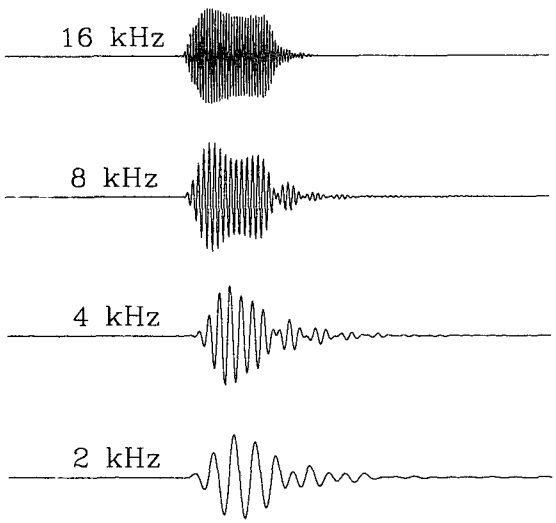

FIG. 5. The AATE replica pulses used in the multidimensional matched filter. The pulses were recorded 100 m from the transmitter, then numerically propagated to 6.43 km by correcting for geometric spreading and chemical absorption (the formula of Francois and Garrison 1982 was used).

balanced winch system. The counterbalance consisted of a free and a motorized pulley, cabling, and weights. The entire assembly was designed to provide a stable, low acoustic noise system that could be driven up and down under computer control. The receiving transducers were supported on a Kevlar line attached via rubber vibration isolators to a plastic coated steel cable that ran over the pulleys. The steel cable came up through a 36 inch hole in the ice, ran over the free pulley, across to the motorized pulley, and down through a second 16 inch hole through the ice for the counterbalance. The two pulleys were separated by nearly 3 m. Suspended at the ends of the cables were 311 kg weights. The weights were carefully balanced so that the motor needed only to overcome the inertia, the drag, and the differential length of cable in the system. The winch, as described in the previous section, was under computer control. The winch position was monitored using an incremental shaft encoder mounted on the free pulley. An optical switch sensed a mark on the cable on each cast. The computer algorithm used the sense information to eliminate creep in the "zero" position of the transducer. The total time between casts was about 5 minutes.

The pulses were received by the three vertically spaced transducers suspended on the winch cable and the single horizontally spaced transducer. A diagram of the received signal hardware is shown in Fig. 6. Each receiving transducer on the winch cable consisted of four elements separated by 4.8 cm. The beam patterns of these transducers were broad enough to allow no more than 2 dB of loss for the 16 kHz pulses at angles less than 10° and still have some directivity at 2 kHz. The horizontal transducer was a spare and differed somewhat from the other three. This transducer consisted of three elements with element spacing of 5.8 cm. The loss was less than 3 dB for angles less than 10°.

Each receiver contained a 40 dB preamp stage. From the preamps, the connection to the surface receiving electronics and computer was made through twisted pairs of Belden 8412 conductors. The signal cables from

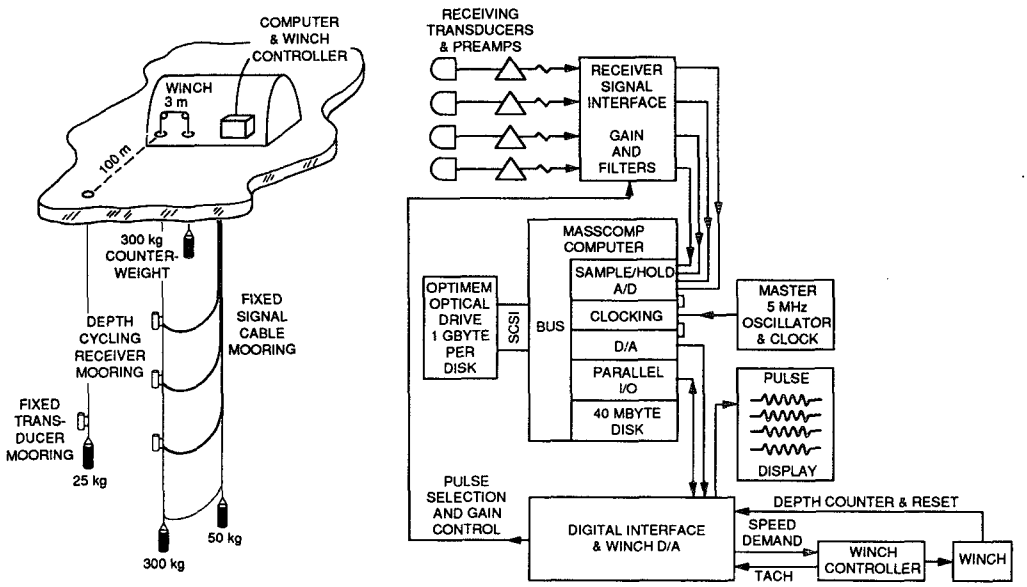

FIG. 6. Diagram of the receiver array, winch, receiver electronics, and computer system.

the transducers were suspended between the receivers and a secondary mooring 25 m behind and to the right of the receiver winch cable (see Fig. 1). Small weights were hung from the signal cables to prevent the cables from streaming and to reduce the effects of current drag. From the stationary transverse receiver, the cable simply ran up its mooring line. Note that, because of limited resources, array tilt and transducer horizontal motion could not be monitored (e.g., by using a pressure sensor at the bottom of the array). Array motion observable in the pulse travel times is discussed in section 4.

The signal conductors were connected to the receiver electronics inside the hut. These electronics provided frequency bandpass filters and attenuation control of the analog signals from the receiver transducers. The signals passed through two gain stages and then into an acoustic-frequency-dependent bandpass filter. The frequency selection and gain in the receiver were controlled by the Masscomp computer to be in lock-step with the transmitter sequence. From these electronics, the signals were connected to sample-and-hold and A/D converters on the host computer.

d. Computer control and data storage

In addition to the winch controller and receiving electronics, three other pieces of electronics hardware were housed in the receiver hut: the clocking hardware described above; a Tektronix 611 x–y display for real-time display of the received pulses; and the Masscomp MC5500 computer that monitored the clocks, controlled the receiving electronics, drove the winch, and digitized and stored the received pulses with intermediate display (see Fig. 6). The computer contained a data acquisition and control processor (DACP®). The software interface to the DACP allows the entire data acquisition and control software to be written in high-level languages (FORTRAN and C). All of the receiving data acquisition and storage, real-time display, monitoring of the external clocks, and winch control were carried out using the single Masscomp. Five DACP modules were used for the experiment: a clocking module containing eight counters; a 12 bit sample-and-hold; an A/D board for digitizing the four input channels of received pulses; a D/A module for real-time output of the received pulses to the display scope; and a 16-line parallel interface module that was used to control the winch and send the frequency select and attenuation settings to the receiving electronics. The parallel interface was also used to monitor the shaft encoder and the winch controller output. Without this system, the experiment would have been impossible under our budgetary and time constraints. (The entire experiment was put together in less than 6 months and was conducted by a party of two scientists and four part-time support engineers.)

The winch cycles were controlled as follows. From rest at the top of each data cast, the software commanded the winch to cycle down so that it was at the selected speed at the correct time and depth for sampling the first pulse in the sequence. After the 400 samples were acquired and stored, the winch was reversed and returned to its rest position. A modified position feedback algorithm was used to control the speed and position of the winch during the data-taking phase. From the upper sampling depth, only the depth separations were maintained; i.e., sampling positions were not adapted during the cast. This approach avoided over-driving the winch. The upper sampling depth was modified cast-to-cast by "learning" a starting time that would get the top receiver closer to the desired starting depth. The upper sampling position then stabilized as the experiment progressed. A plot of depth counter output in Fig. 7 shows nearly constant positions over time, indicating that this scheme worked well. More than a day of depth counts are shown.

Over the 12-day experiment, nearly 10 Gbytes of data were acquired and stored. Because of our inexperience with both the optical drive and the computer acquisition system, a problem occurred at intervals of about an hour that required restarting the data acquisition. After the experiment we learned that the optical disk drive automatically refocuses its optical module at hourly intervals. This problem resulted in some loss

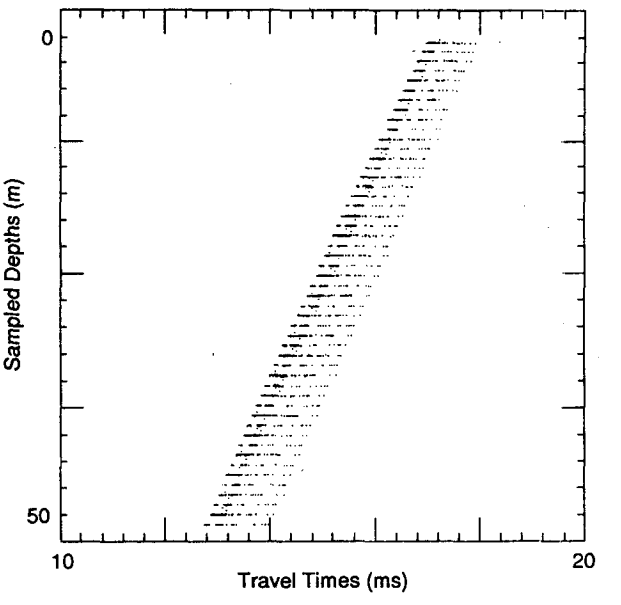

FIG. 7. Representative output of the depth counter during 4 kHz pulse receptions as a function of travel time, for 28 hours during the experiment. For a given sample depth (depth count), the travel times fluctuate over nominally ±0.5 ms (equivalent range change of ±0.75 m). The fact that the depth counts are at discrete counts with very few points in between vertical sample levels on the plot implies that the position feedback algorithm controlling the winch worked well.

of data; however, the amount of data returned was nearly 90% of the possible total, and we feel that the overall system performance was exceptional.

4. Pulse reduction and preliminary results

The equipment used during AATE recorded pulses in depth and time that traversed the 6.43 km range between the transmitter and four receivers. In order to compare the received pulses with acoustic fluctuation theory, the pulses are reduced to sets of amplitudes and travel times. We model the received pulses in the standard way, by assuming that the pulse receptions $r(t)$ consist of time-shifted, amplitude-scaled replicas $s(t)$ contaminated by additive noise $\varepsilon(t)$:

$$r(t) = \sum_{j=1}^{N} a_j s(t - \tau_j) + \varepsilon(t). \quad (1)$$

We call the method used for finding the amplitudes a_j and travel times τ_j a multidimensional matched filter (MDMF). The algorithm as originally implemented is described by Bell and Ewart (1986). Several modifications to the MDMF were made during the processing of the AATE data; a publication describing the use of the algorithm is in preparation. Here we outline the MDMF algorithm used for the AATE pulse reduction. Note that the amplitudes are scaled by the replicas, $s(t)$.

The algorithm solves for the sets of amplitudes $\{a_j\}$ and travel times $\{\tau_j\}, j = 1, \cdots, N$ that minimize the difference between the modeled pulse $\sum_{j=1}^{N} a_j s(t - \tau_j)$ and the received pulse, $r(t)$; i.e., minimize

$$\int_{-\infty}^{\infty} [r(t) - \sum_{j=1}^{N} a_j s(t - \tau_j)]^2 dt, \quad \text{over} \quad \{a_j\}, \{\tau_j\}. \quad (2)$$

Note that this least squares approach is equivalent to a maximum likelihood method when the noise $\varepsilon(t)$ is white over the bandwidth of $s(t)$ and Gaussian. For fixed travel times, $\{\tau_j\}$, minimizing over amplitudes, $\{a_j\}$ is a linear least squares problem. Denote the amplitudes that solve the linear least squares problem by $\{a_j(\tau_j)\}$. The problem given by Eq. (2) is converted to minimizing

$$\int_{-\infty}^{\infty} [r(t) - \sum_{j} a_j(\tau_j) s(t - \tau_j)]^2 dt, \text{ over } \{\tau_j\}. \quad (3)$$

If $\{\hat{\tau}_j\}$ solves the problem given by (3), then $\{a_j(\hat{\tau}_j)\}$ is the solution for the amplitudes. [See Bell and Ewart (1986) for a full presentation.]

Each AATE pulse frequency has a replica $s(t)$ as shown in Fig. 5. The number of paths, N, is left as a parameter. For each pulse, the algorithm solves the $N = 1$ problem first, then progresses to two paths, and so on. The maximum number of paths solved for AATE was two.

With two paths the remainder function

$$\int_{-\infty}^{\infty} [r(t) - \sum_{j=1}^{2} a_j s(t - \tau_j)]^2 dt$$

was reduced to a value nearly equal to the noise energy in the bandwidth of the replica. Using two paths also ensured that, when multipaths were present, the solution would be obtained in an optimal way. In fact, the pulse receptions were usually fit by a single path as anticipated from the ray traces. In tests using more than two paths, additional path amplitudes were much less than the main path amplitude and represented a fitting of noise present during the pulse reception.

The MDMF algorithm is efficient, a requirement because the AATE dataset is large. Nominal analysis times were from 1 to 2 s per pulse, only a factor of 2 to 4 of real time. An initial pass through the dataset revealed occasional 2π jumps in phase. A constrained algorithm was developed to remove the jumps. A search was made limited to a wavelength of the unconstrained path. Using a simple differential detector, jumps were detected and displaced back to be less than 2π; the jumps usually occurred where the signal-to-noise ratio was low. The method used for pulse analysis was checked for accuracy using a network-based matched filter (Bell and Reynolds 1989). By removing the 2π jumps, we were able to maintain the accuracy of fully modulated matched filter processing. The designed resolution of the method was to be less than an eighth of the digitization rate ($1/8 \times 15\ \mu s = 1.9\ \mu s$), and much better than this was achievable in simulation. By examining preliminary travel time spectra at the Nyquist frequency, the actual resolution is less than 7 μs. All pulse reduction has been completed.

Preliminary results from the experiment are shown in Fig. 8. The single path travel times from the top position of the array are shown in the upper part of the figure. The pulse travel times are the measurements one would obtain from a single moored transducer. The information in two dimensions, in the middle and lower part of Fig. 8, was measured from the three depth-cycled receiving transducers. The 2 kHz travel times are shown, with the 8 kHz intensities below. (The other frequencies are similar.)

The example results shown in Fig. 8 allow us to make some final comments regarding array motion. The 2 kHz travel times shown are the measured travel times corrected for clock drift (shown in Fig. 3) and window time changes and with the temporal-averaged travel times for each depth removed. The goal of the experiment is the removal from the measurements of all deterministic effects. As mentioned above, in situ sensors did not monitor the depth of the transducers. We can only estimate motion effects from the travel time

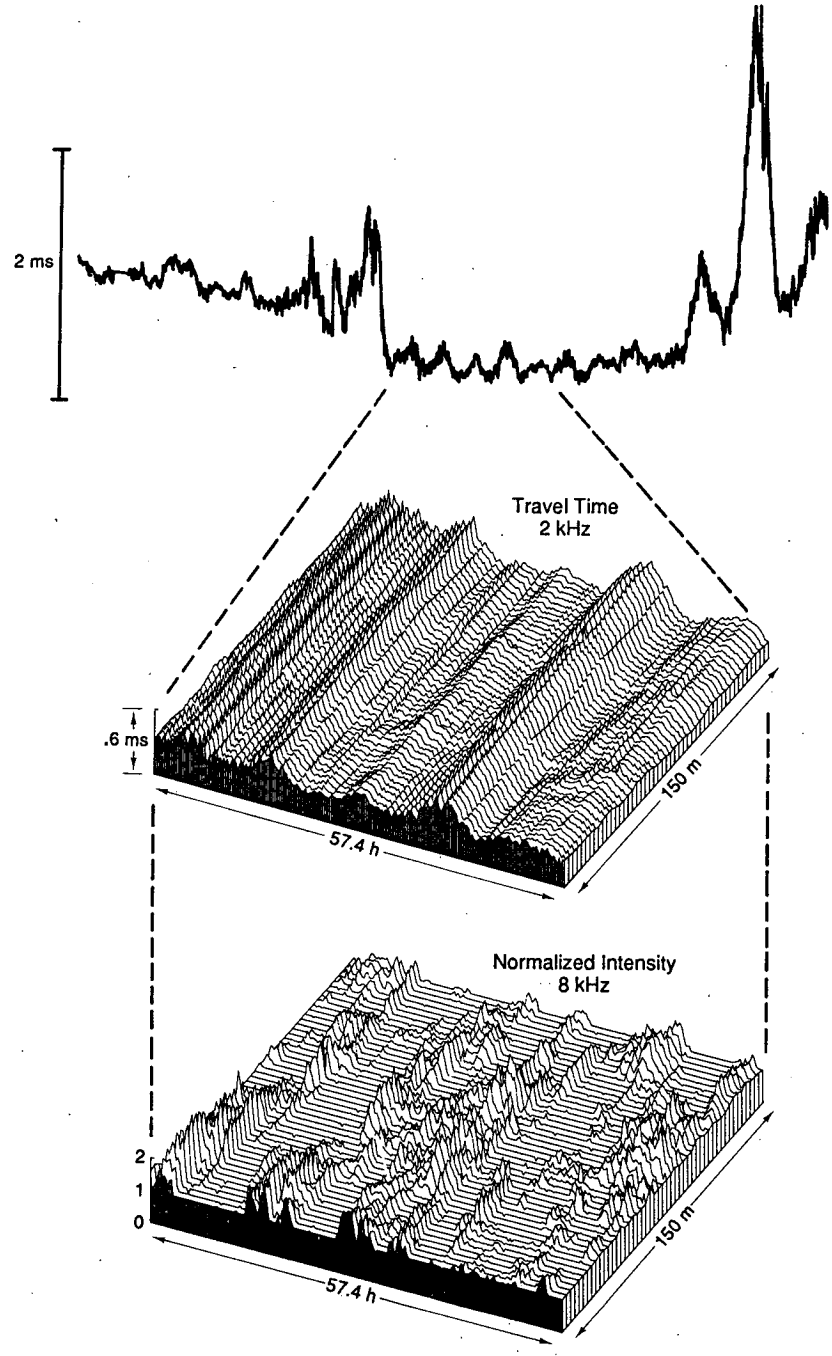

FIG. 8. An example of data from AATE. The top curve shows a one-dimensional recording of the 2 kHz travel times taken at a fixed depth. The large travel-time excursions occurred during wind events when ice motion increased. Datasets of this type are recorded in traditional fixed receiver experiments. The depth–time segment taken from the middle of the top dataset is shown in the middle graph. The depth–time intensity series from the 8 kHz pulses is shown at bottom.

data. By using large weights to moor the arrays to the ice, we hoped to minimize array motion. This appears to have been the case except during wind events. Even with the large weights, an array motion caused by the signal cables is detectable in the profile of average travel times. The measurable signal change as the array moves down equals 30 μs (or 4 cm in range); fluctuations on the order of a tenth of this signal are resolvable with

subcorrelation length averaging. There is also a temporal constraint on the desired internal wave signal: changes of periods less than the inertial period (about 12 hours) are those of interest. Outside of wind events the ice canopy appears stable. Papers in preparation that apply the AATE data to the acoustic forward and inverse problems will discuss the source/receiver relative motion further.

5. Discussion and summary

The depth sampling algorithm used during AATE requires a resampling of the data series on a uniform depth–time grid. Statistics calculated from the resampled series will be used to test numerical and theoretical solutions for volume scattering by internal waves and finestructure. This is the direct or forward problem. This approach has guided much of our progress toward predicting acoustic travel time and intensity fluctuation statistics. The inversion of the observed acoustic results to infer the statistics of the medium is also planned. The results from AATE are currently being used in studies of source localization and backpropagation methods.

In summary, novel instrumentation was used in the Beaufort Sea during 1985 to make two-dimensional measurements of acoustic travel times and amplitudes. The experiment, AATE, took place as a part of AIWEX, the Arctic Internal Wave Experiment. The measurements were made by suspending a three-receiver array from the ice platform and using a low noise electric winch to cycle 51 m, resulting in a receiving aperture that spanned 193 to 346 m. The received pulses propagated over a 6.43 km path from remote 2, 4, 8, and 16 kHz transmitters suspended at 153 m depth. The recorded pulses represent a data return of nearly 90% and will be useful in testing volume fluctuation theory for travel time and intensity fluctuations produced by arctic internal waves and finestructure. Eventually the measurements themselves will be used to obtain the statistics of the intervening medium.

Acknowledgments. We are grateful for the advice and constant support of our colleague and co-investigator Barry Uscinski of the University of Cambridge. The engineering support by Gordon Snowball and Peter Hebbron (Marconi Underwater Systems, Cambridge, U.K.) and the winch were provided by Marconi through the support and encouragement of Alistair Johnson, Director. The efforts of John Okerlund, Mike Welch, and the AIWEX field team headed by Andy Heiberg were invaluable. Support for this work was provided by the Office of Naval Research.

REFERENCES

Bell, B. M., and T. E. Ewart, 1986: Separating multipaths by global optimization of a multidimensional matched filter. *IEEE Trans. Acoust. Speech Signal Process,* **34,** 1029–1037.

——, and S. A. Reynolds, 1989: A matched filter network for estimating pulse arrival times. *IEEE Trans. Acoust. Speech Signal Process,* in press.

Ewart, T. E., 1976: Acoustic fluctuations in the open ocean—A measurement using a fixed refracted path. *J. Acoust. Soc. Am.,* **60,** 46–59.

——, and S. A. Reynolds, 1984: The Mid-Ocean Acoustic Transmission Experiment, MATE. *J. Acoust. Soc. Am.,* **75,** 785–802.

Francois, R. E., and G. R. Garrison, 1982: Sound absorption based on ocean measurements. Part II: Boric acid contribution and equation for total absorption. *J. Acoust. Soc. Am.,* **72,** 1879–1890.

Levine, M. D., 1983: Internal waves in the ocean: a review. *Rev. Geophys. Space Phys.,* **21,** 1206–1216.

——, C. A. Paulson and J. H. Morison, 1985: Internal waves in the Arctic Ocean: Comparison with lower-latitude observations. *J. Phys. Oceanogr.,* **15,** 800–809.

——, —— and ——, 1987: Observations of internal gravity waves under the arctic pack ice. *J. Geophys. Res.,* **92,** 779–782.

Morison, J. H., 1989: Physical oceanography instrumentation for the polar regions: A review. *IEEE J. Ocean. Eng.,* **14,** 173–185.

Munk, W. H., 1981: Internal waves and small-scale processes. *Evolution of Physical Oceanography.* B. A. Warren and C. Wunsch, Eds., MIT Press, 264–291.

Padman L., and T. M. Dillon, 1987: Vertical heat fluxes through the Beaufort Sea thermohaline staircase. *J. Geophys. Res.,* **92,** 10 799–10 806.

Reynolds, S. A., 1982: The Relation of Acoustic Fluctuations to Environmental Variability at Cobb Seamount: the Direct Approach. Ph.D. dissertation, University of Washington, Seattle, 183 pp. (available from University Microfilms, Ann Arbor, MI).

——, S. M. Flatté, R. Dashen, B. Buehler and P. Maciejewski, 1985: AFAR measurements of acoustic mutual coherence functions of time and frequency. *J. Acoust. Soc. Am.,* **77,** 1723–1731.

Uscinski, B. J., 1985: Range and time dependence of acoustic intensity fluctuations. *Ocean Seismo-Acoustics.* T. Akal and J. M. Bertson, Eds., Plenum, 253–268.

Worcester, P. F., G. O. Williams and S. M. Flatté, 1981: Fluctuations of resolved acoustic multipaths at short range in the ocean. *J. Acoust. Soc. Am.,* **70,** 825–840.